第34卷 第1期 焊 接 学 报 Vol. 34 No. 1
2013年1月 TRANSACTIONS OF THE CHINA WELDING INSTITUTION January 2013

预氧化处理对热障涂层热冲击性能及残余应力的影响

李亚娟[1]， 董 允[2]， 王志平[1]， 柳士强[3]
(1. 中国民航大学 理学院，天津 300300; 2. 东北大学秦皇岛分校 材料科学与工程系，秦皇岛 006604;
3. 河北工业大学 材料科学与工程学院，天津 300130)

摘 要: 采用等离子喷涂工艺在镍基高温合金基体上制备了热障涂层(底层为MCrAlY，面层为$ZrO_2+8\%Y_2O_3$)，通过控制高真空烧结炉的氧分压对涂层进行预氧化处理，分析了预氧化处理对热障涂层热冲击性能和涂层应力状态的影响. 结果表明，预氧化处理提高了粘接层的致密度，涂层组织变得均质化，降低了粘结层由于凸起尖角产生复杂应力的概率; 有效干预热生长氧化物(TGO)的生长过程，降低了TGO的生长速度; 热障涂层残余应力随热冲击次数的增加而增大，但经过预氧化处理的涂层应力增长幅度较缓慢，经过400次热冲击后的残余应力为492.5 MPa，未经过预氧化处理涂层热冲击350次后应力值为650.1 MPa.

关键词: 预氧化处理; 热障涂层; 热生长氧化物; 残余应力
中图分类号: TG162.83 **文献标识码**: A **文章编号**: 0253-360X(2013)01-0037-04


李亚娟

0 序 言

热障涂层广泛用于航空发动机叶片、燃烧室、隔热屏、喷嘴、火焰筒等热端部件，保护基体金属，减少高温部件热氧化，提高发动机效率[1,2]. 典型的热障涂层由MCrAlY(M = Ni，Co，Ni + Co)金属粘结层(bond coat，BC)和低导热率的陶瓷面层(top coat，TC)构成，粘结层的作用是缓解陶瓷面层和基体金属热膨胀系数不匹配，保护基体金属不受氧化和腐蚀. 在高温富氧环境下，粘接层中的Al元素向外扩散，在粘接层表面发生选择性氧化，形成一层热生长氧化物(thermally grown oxide，TGO)，如果TGO是由连续且致密的Al_2O_3组成，可以有效阻止粘接层进一步氧化，延长涂层的使用寿命; 但是粘结层主要采用等离子喷涂工艺(air plasma spray，APS)制备，表面存在大量突起、沟壑、尖角等形貌缺陷，高温富氧环境下缺陷处快速生成不规则的大颗粒氧化物，造成致密的Al_2O_3无法生成，随着服役时间的延长，TGO进一步生长、增厚，Al_2O_3形成的同时也会生成尖晶石类氧化物，造成应力集中，在TGO疏松、不连续(Ni，Co元素等大体积氧化物)部位、TGO与粘接层界面的空洞处、TGO曲率较大处生成裂纹并扩展，导致涂层失效[3-7].

文中采用等离子喷涂工艺制备热障涂层，通过控制高真空烧结炉的氧分压对涂层进行预氧化处理(pre-oxidation treatment，POT)，在MCrAlY金属粘结层表面生成一层致密的Al_2O_3薄膜，进行热冲击失效分析和应力测试，与未进行预氧化处理的试样进行对比，分析了预氧化工艺对TGO的形成及涂层失效的影响.

1 试验方法

涂层基体采用GH4099镍基高温合金，喷涂前用丙酮清洗并喷砂处理. 粘结层采用的MCrAlY粉末名义成分为Ni-12.6Cr-22.0Al-9.0Y-0.6Co; 陶瓷层采用的粉末为8YSZ，即采用$8\%Y_2O_3$作稳定剂的ZrO_2陶瓷粉末.

涂层制备采用PRAXAIR & Tafa公司生产的3710型等离子喷涂系统，采用ABB 2004/16型机械手控制喷涂枪移动，喷涂工艺参数见表1.

表1 等离子喷涂工艺参数
Table 1 Processing parameters of plasma spraying

涂层	电流 I/A	电压 U/V	主气压力 p_1/MPa	载气压力 p_2/MPa	喷涂距离 D/mm
BC	835	38	0.42	0.35	85
TC	850	37	0.42	0.35	72

收稿日期: 2011-11-30
基金项目: 国家自然科学基金资助项目(60879018)

预氧化处理采用高真空烧结炉，工艺为将试样放入高真空烧结炉中，加热到 1 050 ℃，在低氧气氛（$p_0 \approx 10^{-2}$ Pa）中保温 18 h，然后冷却到室温.

将热障涂层试样加热到 1 050 ℃，恒温氧化 30 min 取出，用压缩空气冷却至室温，以此作为一次循环. 失效分析及应力测试采用经过 50 次、150 次、350 次、400 次热冲击后的试样.

采用场发射 LEO1530VP 型扫描电镜观察涂层表面和截面的微观组织形貌，化学成分测试采用 EDAX PHOENIX 能谱仪；采用 D/MAX-2500 型 X 射线衍射仪（XRD）对涂层进行物相分析；采用红宝石荧光光谱（RFS）对热障涂层进行残余应力分析，设备型号为 RENISHAW-200 型光谱仪.

2 试验结果及分析

2.1 预氧化处理后的涂层形貌

图 1 为等离子喷涂和经过预氧化处理后的粘接层表面形貌，由图 1a 可以看出，粘结层表面含有大量呈圆球状的未熔颗粒，造成涂层表面凹凸不平. 等离子的温度至少在 8×10^4 K 以上，理论上可将任何材料熔化，但是 MCrAlY 粉末被气体携带进入等离子火焰到沉积在基体表面，在喷涂焰流中停留的时间仅为 $10^{-1} \sim 10^{-6}$ s，部分喷涂颗粒未被熔化而包埋在涂层表面和内部，造成粘结层表面局部区域起伏过大.

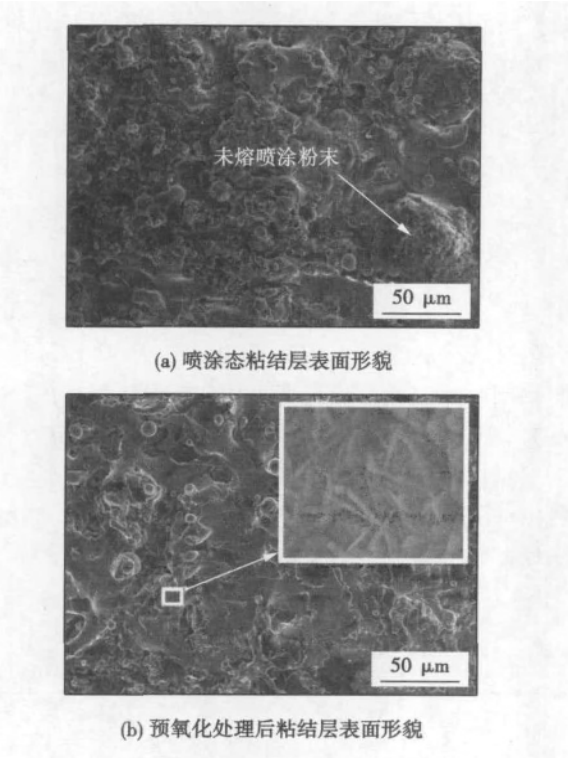

(a) 喷涂态粘结层表面形貌

(b) 预氧化处理后粘结层表面形貌

图 1 粘结层表面形貌（SEM）

Fig. 1 Surface morphologies of bonding coat

由图 1b 可以看出，预氧化处理后的粘结层表面较平整，未发现未熔颗粒，说明预氧化处理使粘结层高度不一致的微观组织变得均质化，改善了因未熔颗粒沉积在涂层中造成涂层表面起伏过大的现象；放大观察发现，粘结层表面生成大量细小的针片状物质. 对其进行能谱分析，结果如图 2 所示，可以看出针片状物质成分主要为 Al 元素和 O 元素. 图 3 为预氧化处理后的粘结层表面 XRD 衍射结果，由图 3 可知，涂层表面仅存在过渡态 θ-Al_2O_3，$AlNi_3$ 的衍射峰，证明针片状物质为 Al_2O_3，该氧化物是在高温状态下选择性氧化产生的，Al 元素优先于粘结层中其它金属元素发生氧化反应生成 Al_2O_3，同时由于真空炉中的氧分压控制在 $10^{-36} \sim 10^{-23}$ MPa 之间，O 元素与粘结层中其它金属元素发生反应后会马上自动分解，因此在此氧分压范围内，预氧化处理产物为单一成分的 Al_2O_3.

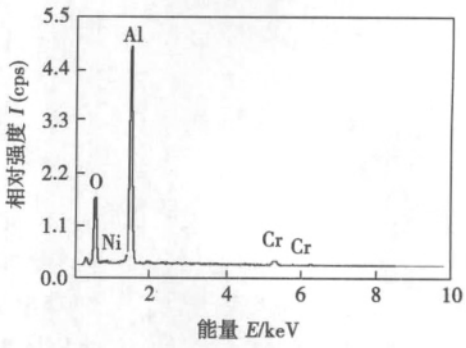

图 2 预氧化处理后粘结层表面针片状物质能谱图

Fig. 2 EDX spectrum of white needles

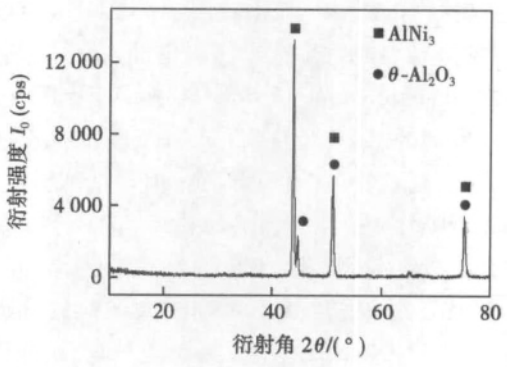

图 3 预氧化处理粘结层表面 XRD 衍射图谱

Fig. 3 XRD patterns of bonding coat after pre-oxidation treatment

2.2 热冲击试验结果及分析

图 4 为等离子喷涂热障涂层的截面形貌. 如图 4a所示，未经过预氧化处理的热障涂层经过 150

次热冲击后 TGO 出现双层结构,说明热冲击过程中,伴随 Al_2O_3 膜生成的同时,Al_2O_3 膜和陶瓷层的界面处也生成了 Cr,Ni 元素的氧化物以及尖晶石类氧化物,在随后的热冲击过程中,混合氧化物层快速生长增厚,空隙增多,引起应力集中,产生裂纹,伴随热冲击次数的增加,裂纹进一步扩展,350 次热冲击后涂层产生大面积剥离(图 4b).

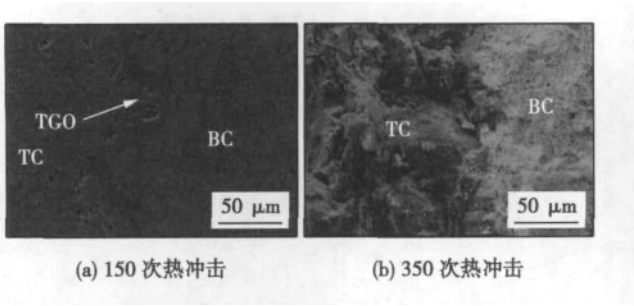

图 4　喷涂态热障涂层热冲击后的截面形貌

Fig. 4　Cross-sectional morphology of plasma coating following thermal cycles

图 5 为经过预氧化处理的热障涂层热冲击后截面形貌. 预氧化处理的热障涂层经过 150 次热冲击,在粘结层与陶瓷层的界面处出现连续的热生长氧化物,即 TGO 层,其形态规则,厚度均匀,没有明显的形貌起伏,陶瓷层内存在一些孔洞和微裂纹,但未出现宏观裂纹(图 5a). 孔洞和微裂纹的出现是由于喷涂过程中沉积不均匀产生孔隙,在热冲击过程中受冷热交替的作用,使陶瓷层内孔隙连接扩展,生成微裂纹,这些微裂纹在热冲击的初期有效降低陶瓷层内应力集中水平[8]. 经过 400 次热冲击,TGO 形貌与经过 150 次热冲击的相比无明显变化,厚度均匀且比较致密,陶瓷层与 TGO 的界面处、TGO 内部未发现明显的孔洞等缺陷(图 5b).

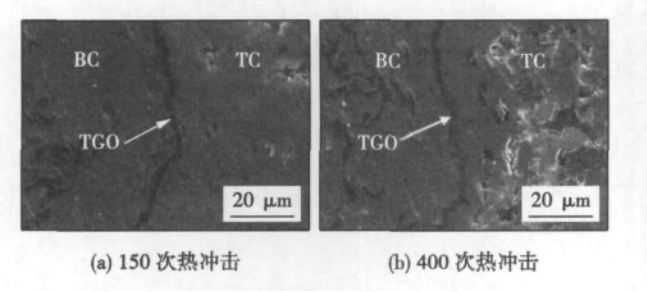

图 5　预氧化处理的热障涂层热冲击后的截面形貌

Fig. 5　Cross-sectional morphology of coating after pre-oxidation treatment following thermal cycles

2.3　涂层的残余应力计算

TGO 最重要的组成相是 Al_2O_3,由于 Cr^{3+} 和 Al^{3+} 的半径相似,两者可以形成固溶体,前者常以杂质的形式存在于 Al_2O_3 中,Cr^{3+} 的荧光谱线受应力影响而发生偏移,通过测量 Cr^{3+} 的频率偏移量就可知 Al_2O_3 晶格所受的应力[9].

假设涂层为平面应力状态,假定 $\sigma_{xx}=\sigma_{yy}=\sigma$,$\sigma_{zz}=0$(其中,$\sigma_{xx}$,$\sigma_{yy}$,$\sigma_{zz}$分别为轴向、径向和法向残余应力). 涂层中任一点的应力与拉曼特征峰 R_2 频移之间的关系为

$$\sigma = 197\Delta\upsilon_{R_2} \qquad (1)$$

式中: 197 为试验测定因子; $\Delta\upsilon_{R_2}$ 为 R_2 的峰值频移.

拉曼光谱法收集得到的等离子热障涂层热冲击试样光谱如图 6 所示. 对测试结果进行分析,获得的测试数据及计算得到的残余应力值见表 2. 应力测试结果显示,预氧化处理的热障涂层经过 50 次,400 次热冲击后残余应力分别为 197.0,492.5 MPa,未经过预氧化处理的热障涂层经过 50 次,350 次热冲击后残余应力分别为 275.8,650.1 MPa. 热障涂层 TGO 的残余应力随热冲击次数的增多而增大,但经过预氧化处理的热障涂层残余应力比喷涂态涂层低了 30% 以上.

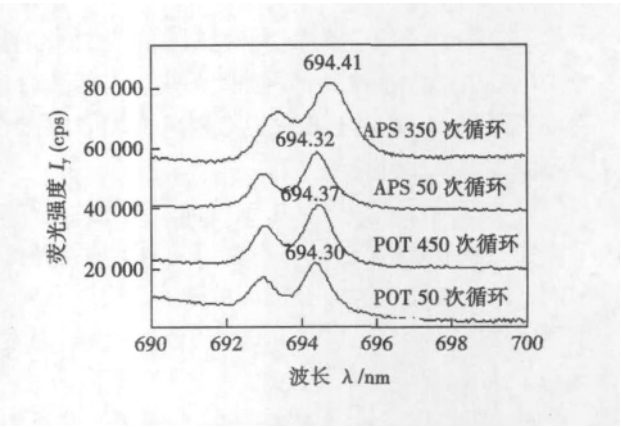

图 6　热障涂层热冲击后的光谱图

Fig. 6　Spectrogram of TBC following thermal cycles

表 2　热障涂层 RFS 测试数据及计算结果

Table 2　RFS data and residual stress of TBC

热冲击次数	R_2 的波长 λ_{R_2}/nm	R_2 的频率 ν_{R_2}/cm^{-1}	R_2 的峰值频移 $\Delta\nu_{R_2}$/cm^{-1}	残余应力 σ/MPa
APS 0 次	694.25	14 404.0	0	0
APS 50 次	694.32	14 402.6	−1.4	−275.8
APS 350 次	694.41	14 400.7	−3.3	−650.1
POT 50 次	694.30	14 403.0	−1.0	−197.0
POT 400 次	694.37	14 401.5	−2.5	−492.5

热冲击过程中,随着热冲击次数的增加,在冷热频繁交替作用下,喷涂态的热障涂层和经过预氧化处理的热障涂层 TGO 层内残余应力都不断增大,但是经过预氧化处理的热障涂层残余应力增长幅度较

喷涂态喷涂热障涂层缓慢. 这是由于 TGO 的应力水平与其生长规律有关,随着热冲击次数的增加,TGO 逐渐生长变厚,产生较大的残余应力. 经过预氧化处理的热障涂层因 Al_2O_3 膜的提前生成,降低了粘接层的氧化速度,从而降低了 TGO 由于不断生长增厚而产生的残余应力,同时抑制有害氧化物的生成,避免了因尖晶石类氧化物的生成而出现的应力集中现象;对喷涂态涂层进行预氧化热处理消除了等离子喷涂在沉积过程中产生的残余应力,提高了涂层致密度,粘结层的微观组织变得均质化,缓解了粘结层在凸起尖角处产生的复杂应力. 因此预氧化处理改善了热障涂层热冲击过程中 TGO 层内的应力状态.

3 结 论

(1) 采用等离子喷涂工艺制备的热障涂层经过350 次热冲击后,在交变应力与热生长应力的双重作用下,涂层出现贯穿裂纹,涂层失效. 经过预氧化处理的热障涂层,经过 400 次热冲击后热障涂层依然完好.

(2) 喷涂态的热障涂层和经过预氧化处理的热障涂层随着热冲击次数的增加,TGO 层内的残余应力都不断增大,预氧化处理后涂层应力增长幅度小于喷涂态等离子热障涂层.

(3) 对喷涂态热障涂层进行预氧化热处理提高了涂层致密度,粘结层的微观组织变得均质化,降低了由于凸起尖角产生复杂应力的概率. 同时有效地干预了 TGO 的生长过程,降低了 TGO 的生长速度,减少了 TGO 层应力集中现象.

参考文献:

[1] 徐庆泽, 梁春华, 孙广华, 等. 国外航空涡扇发动机涡轮叶片热障涂层技术发展[J]. 航空发动机, 2008, 34(2): 52-56.
Xu Qingze, Liang Chunhua, Sun Guanghua, *et al*. Development of thermal barrier coating for foreign turbofan engine turbine blade [J]. Aeroengine, 2008, 34(2): 52-56.

[2] Maricocchi A, Bartz A, Wortman D. PVD TBC experience on GE aircraft engines [J]. Journal of Thermal Spray Technology, 1997, 6(2): 193-198.

[3] Martina D F, Alessio F, Alessandro L, *et al*. Isothermal oxidation resistance comparison between air plasma sprayed, vacuum plasma sprayed and high velocity oxygen fuel sprayed CoNiCrAlY bond coats [J]. Surface and Coatings Technology, 2010, 204(15): 2499-2503.

[4] Leonardo A, Josep A P, George E K, *et al*. Oxidation behavior of HVOF sprayed nanocrystalline NiCrAlY powder [J]. Materials Science and Engineering: A, 2002, 338(1/2): 33-43.

[5] 张丽娟, 林晓娉, 刘春阳, 等. 高速微粒轰击对热障涂层热生长氧化物生长过程的影响[J]. 材料热处理学报, 2009, 30(3): 182-186.
Zhang Lijuan, Lin Xiaoping, Liu Chunyang, *et al*. Effect of high-speed fine particles bombarding on thermally grown oxide growth process of thermal barrier coatings [J]. Transactions of Materials and Heat Treatment, 2009, 30(3): 182-186.

[6] Picas J A, Forn A, Matthus G. HVOF coatings as an alternative to hard chrome for pistons and valves [J]. Wear, 2006, 261(5/6): 477-484.

[7] Wellman R G, Nicholls J R. Erosion, corrosion and erosion-corrosion of EB PVD thermal barrier coatings [J]. Tribology International, 2008, 41(7): 657-662.

[8] Sfar K, Aktaa J, Munz D. Numerical investigation of residual stress fields and crack behavior in TBC systems [J]. Materials Science and Engineering: A, 2002: 333(1/2): 351-360.

[9] Maurice G, Jordan E, Vaidyanathan K, *et al*. Bond strength, bond stress and spallation mechanisms of thermal barrier coatings [J]. Surface and Coatings Technology, 1999, 120/121: 53-60.

作者简介: 李亚娟,女,1978 年出生,博士,讲师. 主要从事材料改性及失效机理研究工作. 发表论文 10 余篇. Email: yj-li@cauc.edu.cn

indicates that the flow behavior of filler metal in unparalleled clearance is influenced by the combined effect of ultrasonic induced gap-filling action and capillary action.

Key words: ultrasonic brazing; high-speed video camera investigation; gap; filling gap; dynamics

Effect of pre-oxidation treatment on thermal shock resistance and residual stress of thermal barrier coating LI Yajuan[1], DONG Yun[2], WANG Zhiping[1], LIU Shiqiang[3] (1. College of Science, Civil Aviation University of China, Tianjin 300300, China; 2. Department of Materials Science and Engineering, Northeastern University at Qinhuangdao, Qinhuangdao 066004, China; 3. School of Materials Science and Engineering, Hebei University of Technology, Tianjin 300130, China). pp 37 - 40

Abstract: The thermal barrier coating by taking MCrAlY as bonding coating and $ZrO_2 + 8\% Y_2O_3$ as top coating were deposited on the nickel-based super-alloy by air plasma spraying. Pre-oxidation treatment was carried out on the thermal barrier coatings by controlling the oxygen pressure in high vacuum sintering furnace. Then, the effects of pre-oxidation treatment on the thermal shock resistance and residual stress were investigated, respectively. The results show that pre-oxidation treatment improves the density of bonding coating, which makes it uniform and reduces the probability of complex stress caused by convex point in interface area. Meanwhile, pre-oxidation treatment interferes the growth process of thermally grown oxide (TGO), reduces the TGO growth rate and the stress concentration of coating. Residual stress increases with the increasing of thermal cycles. However, pre-oxidation treatment can slow down the increasing rate of residual stress. The residual stress of 650.1 MPa can be reached after 350 thermal cycles without pre-oxidation, while the residual stress is only 492.5 MPa after 400 thermal cycles with pre-oxidation.

Key words: pre-oxidation treatment; thermal barrier coating; thermally grown oxide; residual stress

Calibration of relative position and orientation between robot and positioner based on spheres fitting method ZHU Xiaopeng, ZHANG Ke, TU Zhiqiang, HUANG Jie (Shanghai Key Laboratory of Laser Manufacturing & Material Modification, Shanghai Jiao Tong University, Shanghai 200240). pp 41 - 44

Abstract: A method to calibrate the relative position and orientation between robot and positioner was presented by fitting sphere based on the least square method. Firstly, the positioner rotates or tilts to different positions, and the position data of TCP were recorded in the same time. The optimal sphere was fitted by the least square method, and the origin of base coordinate frame of the positioner was calculated. Secondly, several points were recorded in the same way to calculate the vectors of axis. In order to avoid the effects of causal factors, the concept of deviation rate was presented to verify the accuracy of the marked points. Experiments show that this method can reduce the random error and avoid the effects of causal factors, which has high precision.

Key words: robot; laser cladding; calibration; sphere fitting method; least square method

Spectrum of MIG arc at different welding parameters LI Zhiyong, ZHANG Wenzhao, LI Yan, DING Jingbin (Welding Research Center, North University of China, Taiyuan 030051, China). pp 45 - 48, 52

Abstract: The droplet transfer mode and arc length variation are the significant factors affecting the radiation intensity of arc plasma for MIG welding. It is critical to understand the regularity of the radiation fluctuation in application in industry control of the welding process. Therefore, the spectrum of MIG arc radiation was collected with a spectrometer based system. The spectrums of welding processes at different welding parameters were analyzed to study the regularity of the radiation variation. Based on the arc physics, the spectral information combining with the droplet transfer mode was used to get a better understanding of the arc radiation. The results show that the arc spectrum with its distinct distribution is different at different welding parameters. The MIG arc emits wavy radiation due to droplet transfer. The spectral signals in different spectrum bands, such as ultraviolet, visible and near infrared band, have totally different variation characteristics during different instance of the droplet transfer.

Key words: arc spectrum; welding parameter; MIG welding; droplet transfer

Microstructure and properties of diffusion bonded interface of titanium-copper interlayer-carbon steel composite tube LIU Deyi, CAI Jianwei, REN Ruiming (School of Materials Science and Engineering, Dalian Jiaotong University, Dalian 116028, China). pp 49 - 52

Abstract: The composite tube of titanium/steel was prepared by the drawing and inner pressure diffusion technique by using Cu foil as an interlayer. The interface microstructure, fractured surface and components were investigated with OM, SEM, XRD and EDS. The bonding strength of the interface was studied by shear test. The results show that the metallurgical bonding of titanium and steel was obtained by the drawing and inner pressure diffusion technique with copper foil as an interlayer. The interface components analysis show that the elements diffusion was found between the titanium/copper interface and the diffusion layer was formed. The thickness of the diffusion layer increased with increasing of diffusing time. The Fe-Ti brittle compound was prevented by using copper interlayer at lower diffusion temperature. The shear strength of titanium/steel interface firstly increased and then decreased with diffusion temperature increasing. Copper interlayer can improve the shear strength significantly, and the maximum shear strength can reach 310 MPa.

Key words: titanium/steel; interlayer; diffusion bonding; bonding strength

Effect of Zn on formation of voids on Sn*x*Zn/Cu interface YANG Yang[1], LU Hao[1,2], YU Chun[1], CHEN Junmei[1], CHEN Zhenying[1] (1. School of Materials Science and Engineering, Shanghai Jiaotong University, Shanghai 200240, China; 2. Key Laboratory of Shanghai Laser Manufacturing and Materials Modification, Shanghai Jiaotong University, Shanghai 200240, China). pp 53 - 56

Abstract: The effect of Zn on formation of Kirkendall voids on the interface was studied through the reaction between Sn*x*Zn solders ($x = 0, 0.2\%, 0.5\%, 0.8\%$) and the electroplated Cu substrate. During the thermal aging of Sn/Cu joints, a number of Kirkendall voids were formed in the Cu_3Sn layer and on the Cu_3Sn/EPC interface. With the increase of Zn content in solder, the growth of Cu_3Sn layer was greatly suppressed, and the formation of Kirkendall voids was effectively inhibited. The concentration of Zn on the reaction interface also significantly increased. Zn participated in the interface reaction, (Cu,